Hindawi
Mathematical Problems in Engineering
Volume 2018, Article ID 6412030, 10 pages
https://doi.org/10.1155/2018/6412030

Research Article

Symmetrical Workspace of 6-UPS Parallel Robot Using Tilt and Torsion Angles

Yanli Liu,[1,2] **Hongtao Wu**,[1] **Yuxuan Yang**,[1] **Shangyuan Zou**,[3] **Xuexiang Zhang**,[1] **and Yaoyao Wang**[1]

[1]*College of Mechanical and Electrical Engineering, Nanjing University of Aeronautics & Astronautics, Nanjing 210016, China*
[2]*Department of Mechanical Engineering, Jiangsu College of Safety Technology, Xuzhou 221011, China*
[3]*Department of Automotive Engineering, Jiangsu College of Safety Technology, Xuzhou 221011, China*

Correspondence should be addressed to Yanli Liu; mee_liuyanli@126.com

Received 21 March 2018; Revised 10 May 2018; Accepted 22 May 2018; Published 21 June 2018

Academic Editor: Oscar Reinoso

For the fast and efficient closed-loop real-time feedback control of 6-UPS parallel robot (6-UPS), a novel high efficiency calculation of the workspace is proposed and investigated. As a typical Nearly General Platform (NGP), 6-UPS has good symmetries. The symmetries effectively reduce computational cost and improve computational efficiency in the kinematics, singularity, dynamics, and optimization. To scrupulously demonstrate the symmetries of workspace, a novel algorithm is proposed. The modified Euler angles (T&T angles) are employed to represent the orientation matrix of 6-UPS, the inverse kinematics is analyzed, and the workspace of 6-UPS is obtained using the discretization algorithm. Meanwhile, the symmetries of the total orientation workspace are also proved. Compared with the traditional methods, the total orientation workspace reduces 5/6 computation cost, which means that the corresponding computation efficiency is increased by 6 times. Through theoretical and numerical calculations, the symmetries of the total orientation workspace of 6-UPS are verified. The proof of the symmetries lays a solid foundation for improving the computational efficiency of kinematics, dynamics, and control of 6-UPS.

1. Introduction

The analysis of workspace is very important for designing and analysis of 6-UPS. Besides, workspace of 6-UPS is relatively limited with respect to serial robot in similar size [1]. And the structure parameters of 6-UPS have influence on the workspace. Therefore, they should be carefully optimized in order to satisfy certain tasks. The optimization leads to the problem of gauge and evaluation of workspace. Merlet [1] categorized methods of calculating workspace into 3 types, i.e., geometrical approach, discretization method, and numerical methods. This paper focuses on benefits of symmetries in discretization method.

Obviously, if the workspace is symmetrical, the computational cost is effectively reduced. The number of the poses which is tested to see whether it belongs to the workspace is reduced, and even the location of the inscribed regular workspace is easier to be determined. Generally, the workspace of 6-UPS is irregular, while we need to consider some regular geometry, like a cube, a cylinder, or a sphere, as the effective workspace. Yunjiang Lou [2] regarded an effective regular workspace. He chooses the largest inscribed cubic workspace in the real workspace. Also, some researchers choose cylindrical workspace [3] and spherical workspace [4]. The regular workspace is symmetrical. If the real workspace is symmetrical, then, when calculating the regular inscribed geometry, the process of finding the location of the geometry is simplified. For example, if the workspace is rotational symmetry about z-axis, then the geometrical center of the regular symmetrical geometry should be on z-axis.

Many classical and widely used 6-UPS have symmetrical structures. Therefore, the proof of the symmetry is beneficial. Some researchers have studied the relative characteristics. Jingshan Zhao [5] proposed an analogous symmetric theorem of workspace for spatial 6-UPS with identical kinematic

chains. The theorem has a precondition that every kinematic chain is collinear. Then, Jingshan Zhao [6] used group theory to prove the 3-dimension reachable workspace of 6-UPS with symmetrical structure possesses corresponding symmetry without the previous precondition. The group theory is a deep and general representation method and covers many kinds of parallel mechanisms. Furthermore, the symmetry group theory is applied in inverse kinematic identification of parallel mechanisms [7]. However, the group theory is only used in reachable workspace. The group theory is defined as either the position P is known and the orientation matrix R is unknown or, otherwise, the reverse. However, in reality, the tasks of parallel robots, machine tools, and space simulators usually require a 6-dimensional motion. As a consequence, the reachable workspace is not enough for analyzing 6-UPS, while 6-dimension total orientation workspace is more suitable. Therefore, the symmetrical characteristics of total orientation workspace are discussed in this paper.

The representation of orientation is a key point in the symmetrical workspace. Different representations have direct influence on the calculation and analysis of the workspace. The choice of orientation parameters is the most crucial issue in the analysis of 6-UPS [8]. The calculation cost of algorithm is different along with the parameterization. Therefore, it should be cautious. The main idea of choice of parameters is to make the symmetries of 6-UPS easy to be explicitly expressed. The idea is realized by the effective parameterization of mapping relations between 6-dimensional inputs and 6-dimensional outputs of 6-UPS. Generally, the widely used representations are Z-Y-Z Euler Angles, RPY angles [9], direction cosines [10], and quaternion [5]. However, the symmetry is difficult to be expressed. In this paper, T&T angles named as modified Euler angles [11] are chosen for the orientation matrix. Its parameters possess physical meanings and it is the foundation in the proof of the symmetries. This new representation of orientation was firstly proposed by Bonev and Ryu [12]. Later, Huang [13] and Crawford [14] employed it. Then, Bonev [11] analyzes its advantages in 6-UPS, such as the direct geometrical interpretations of three parameters, the close relationship with the motion of CNC machine tool, and the simple and intuitive orientation representation. Bonev and Gosselin address the advantages in analysis result of the singularity and workspace of symmetrical spatial 6-UPS [15, 16] by employing T&T angles. Besides, there exist more benefits of T&T angles than the group theory, such as intuitively, concisely, and clearly. That is, it only needs to change the coordinates of position and orientation which facilitate to program and calculate. Furthermore, it only needs vectors, matrices, additions, multiplications, and their combinatorial operation. These benefits are easy for the computer to compute.

In this paper, the aforementioned aspects are addressed. The symmetries of 6-UPS, mainly include workspace, are proved and verified. The T&T angles are used to represent the orientation matrix. Combining the discretization algorithm the reachable workspace is solved. The workspace is extended to the total orientation workspace. Therefore, the symmetries of the total orientation workspace are discovered, proved, and compared with the RPY angles representation method.

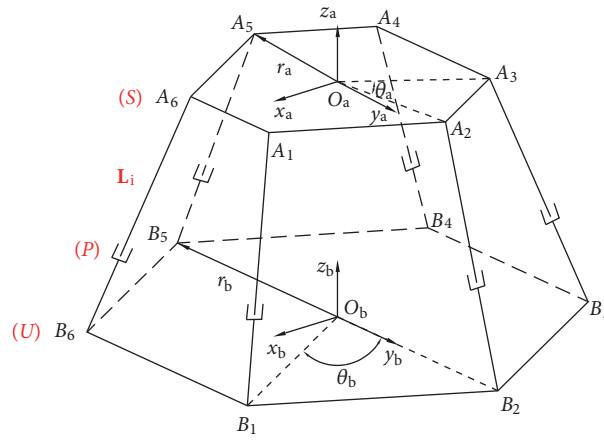

Figure 1: The structure diagram of 6-UPS.

Accordingly, the contributions of this paper are as follows. (1) The T&T angles are discovered to represent the orientation matrix leading to the symmetries of the total orientation workspace. (2) Based on (1), the symmetries are proved for the total orientation workspace of 6-UPS. The symmetries reduce down the computational time and speed-up 6 times computational efficiency for the closed-loop real-time feedback control of 6-UPS.

This paper is organized as follows. In Section 2, the preliminary definitions is presented and detailed. In Section 3, the proof and analysis of symmetries are done. Numerical validations and discussion are presented in Section 4. Finally, Section 5 summarizes this paper.

2. Preliminary Definitions

2.1. Kinematics Fundamentals. The classical 6-UPS consists of two platforms and six legs which connect the two platforms, as shown in Figure 1. One passive joint connecting the leg L_i and the base platform is universal joint U. The other passive joint connecting the leg L_i and the mobile platform is spherical hinge S. The active joint is prismatic joint P fixed on each leg. The desired movement of mobile platform is obtained by adding drive on each P joint. A_i and B_i are the center of spherical joint S and universal joint U, respectively. All A_i and B_i are restricted to a plane, respectively, that is, this 6-UPS belongs to the plane type. $O_a x_a y_a z_a$ and $O_b x_b y_b z_b$ are the coordinate system fixed on the mobile platform and the base platform, respectively. O_a is the center of the mobile platform and also the origin of the moving frame $\{O_a\}$. O_b is the center of the base platform and also the origin of the base frame $\{O_b\}$. z_a and z_b axes are perpendicular to the belonged plane, respectively.

The pose of the moving frame with respect to the base frame is regarded as the end-effector of the mechanism. The structure is symmetrical; i.e., the six kinematic chains are identical and the six link joints on each platform are on the vertices of a symmetrical hexagon. Also the link joints of the two platforms are inscribed in two circles, respectively, as shown in Figure 2.

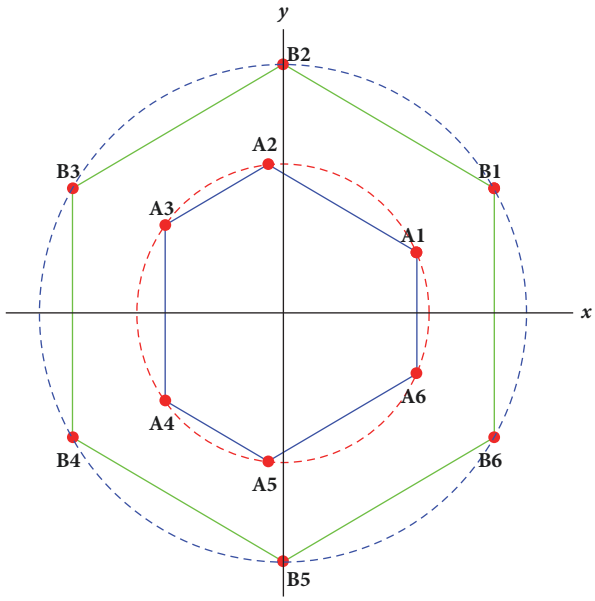

Figure 2: Diagrams of the two frames.

2.2. Representation of Orientation Matrix. The T&T angles are employed to represent the orientation matrix **R**. Literally, the T&T angles consist of two parts, i.e., tilt and torsion. Three parameters are included in this representation. Two of three parameters determine the tilt and the third parameter determines the torsion. As shown in Figure 3, we first rotate the frame $\{i\}$ about the base z_i-axis by an angle ϕ, then about the y_i-axis by an angle θ, then about the z_j-axis by an angle $-\phi$, and finally about the new z_k-axis by an angle σ.

The new orientation angles, $[\phi, \theta, \sigma]$, are called azimuth, tilt, and torsion, respectively. The orientation matrix, thus, is easily gotten as follows:

$$\begin{aligned}\mathbf{R}(\phi,\theta,\sigma) &= \mathbf{R}_z(\phi)\,\mathbf{R}_y(\theta)\,\mathbf{R}_z(-\phi)\,\mathbf{R}_z(\sigma)\\ &= \mathbf{R}_z(\phi)\,\mathbf{R}_y(\theta)\,\mathbf{R}_z(\sigma-\phi)\\ &= \begin{bmatrix} c\phi c\theta c\varphi - s\phi s\varphi & -c\phi c\theta s\varphi - s\phi c\varphi & c\phi s\theta \\ s\phi c\theta c\varphi + c\phi s\varphi & -s\phi c\theta s\varphi + c\phi c\varphi & s\phi s\theta \\ -s\theta c\varphi & s\theta s\varphi & c\theta \end{bmatrix}\end{aligned} \tag{1}$$

where $c\phi = \cos\phi$, $s\phi = \sin\phi$, $c\theta = \cos\theta$, $s\theta = \sin\theta$, $c\varphi = \cos\varphi$, $s\varphi = \sin\varphi$, and $\varphi = \sigma - \phi$.

The first three rotations are in fact the tilt about a vector **u** by θ, where **u** is a vector in x-y plane and the angle from base y_i-axis to it is ϕ. The direct cosine about the rotational axis **u** is easy to be validated to be equivalent to three rotations; i.e.,

$$\mathbf{R}_u(\theta) = \mathbf{R}_z(\phi)\,\mathbf{R}_y(\theta)\,\mathbf{R}_z(-\phi) \tag{2}$$

The last rotation is the torsion.

2.3. Analysis of Workspace

2.3.1. Solution of Total Orientation Workspace Using Discrete Method. In this paper, the discrete method is used to solve the total orientation workspace. The position is sampled discretely in a given range of workspace. What is more, the position point is sampled during the set of orientation angles. Therefore, the six lengths of legs, input coordinates, are obtained by the position and orientation given by the inverse kinematics, as shown in

$$L_i = \left|\mathbf{u}_\mathrm{P} + \mathbf{R}(\mathbf{u}_\mathrm{R})\cdot\mathbf{a}_i - \mathbf{b}_i\right| \quad i = 1,\ldots,n \tag{3}$$

where L_i is the length of the ith leg, $\mathbf{u}_\mathrm{P} = [x, y, z]^\mathrm{T}$ is the position vector of the mobile platform in the base frame $\{O_b\}$, $\mathbf{R}(\mathbf{u}_\mathrm{R}) = \mathbf{R}_z(\phi)\mathbf{R}_y(\theta)\mathbf{R}_z(\sigma - \phi)$ is the orientation matrix, $\mathbf{a}_i = [x_{ai}, y_{ai}, z_{ai}]^\mathrm{T}$ is the position vector which denotes the vertices of the mobile platform in the moving coordinate system, and $\mathbf{b}_i = [x_{bi}, y_{bi}, z_{bi}]^\mathrm{T}$ is the position vector which denotes the vertices of the fixed base in the static coordinate system. Because the vertices of the mobile platform and base platform are all arranged in a plane, the z-axis component of a_i and b_i is 0. Thus, $\mathbf{a}_i$ and $\mathbf{b}_i$ can be expressed as $\mathbf{a}_i = [x_{ai}, y_{ai}, 0]^\mathrm{T}$ and $\mathbf{b}_i = [x_{bi}, y_{bi}, 0]^\mathrm{T}$.

For Figure 1, the vectors along the axis of ith leg between 6 pairs of corresponding vertices on the upper and lower platforms are easily represented as follows:

$$\mathbf{L}_i(\mathbf{u}) = \mathbf{u}_\mathrm{P} + \mathbf{R}(\mathbf{u}_\mathrm{R})\,\mathbf{a}_i - \mathbf{b}_i \quad i = 1, 2, \ldots, \mathrm{n} \tag{4}$$

where $\mathbf{L}_i(\mathbf{u})$ is the vector of the ith leg and

$$\mathbf{L}(\mathbf{u}) = \left[\left|\mathbf{L}_1(\mathbf{u})\right|, \left|\mathbf{L}_2(\mathbf{u})\right|, \ldots, \left|\mathbf{L}_n(\mathbf{u})\right|\right] \tag{5}$$

where $|\mathbf{L}_i(\mathbf{u})|$ are the lengths of six legs.

Then to determine whether $|\mathbf{L}_i(\mathbf{u})|$ meet the following constraints, one has the following:

$$L_\mathrm{min} < \left|\mathbf{L}_i(\mathbf{u})\right| < L_\mathrm{max}, \quad i = 1, 2, \ldots, n \tag{6}$$

In Table 1, vectors $\mathbf{a}_1, \ldots, \mathbf{a}_6$ and vectors $\mathbf{b}_1, \ldots, \mathbf{b}_6$ represent the vertices of the mobile platform and the vertices of the fixed base, respectively. In general, the radius of the mobile platform circumcircle is assumed to be r_a, while the radius of the fixed base circumcircle is assumed to be r_b. And θ_a and θ_b are center semiangles corresponding to the short side of platform, respectively.

2.3.2. Definition of Workspace. The discretization method is often used to calculate the workspace of 6-UPS. The main idea is to calculate the values of generalized coordinates, like active and passive joint values, from a given pose by inverse kinematics of 6-UPS. Then the values of generalized coordinates are checked with the constraints, like translation and rotation ranges of joints and collision constraints. If the values satisfied all the constraints, then the pose belongs to the reachable workspace.

The generalized coordinates, $\mathbf{q} = [q_1, q_2, \ldots, q_{n_q}]^\mathrm{T} \in \mathbf{R}^{n_q}$, represent the position and orientation of every component in the mechanism. Usually, the motion of the mechanism is controlled by some values of the generalized coordinates, like the six active prismatic joints of 6-UPS. Those coordinates constitute input coordinates, represented as

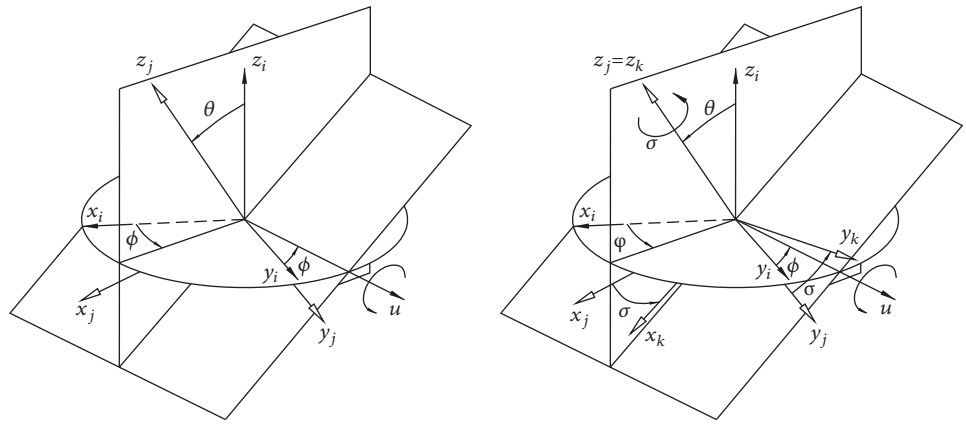

Figure 3: Two successive rotations that define the T&T angles: (a) tilt; (b) torsion.

Table 1: Vertex parameters of two platforms.

	a_{xi}	a_{yi}	b_{xi}	b_{yi}
1	$r_a \cos(\theta a)$	$r_a \sin(\theta a)$	$r_b \cos(\theta b)$	$r_b \sin(\theta b)$
2	$r_a \cos(2\pi/3 - \theta a)$	$r_a \sin(2\pi/3 - \theta a)$	$r_b \cos(2\pi/3 - \theta b)$	$r_b \sin(2\pi/3 - \theta b)$
3	$r_a \cos(2\pi/3 + \theta a)$	$r_a \sin(2\pi/3 + \theta a)$	$r_b \cos(2\pi/3 + \theta b)$	$r_b \sin(2\pi/3 + \theta b)$
4	$r_a \cos(4\pi/3 - \theta a)$	$r_a \sin(4\pi/3 - \theta a)$	$r_b \cos(4\pi/3 - \theta b)$	$r_b \sin(4\pi/3 - \theta b)$
5	$r_a \cos(4\pi/3 + \theta a)$	$r_a \sin(4\pi/3 + \theta a)$	$r_b \cos(4\pi/3 + \theta b)$	$r_b \sin(4\pi/3 + \theta b)$
6	$r_a \cos(-\theta a)$	$r_a \sin(-\theta a)$	$r_b \cos(-\theta b)$	$r_b \sin(-\theta b)$

$\mathbf{v} = [v_1, v_2, \ldots, v_{n_v}]^T$, while the pose of end-effector is defined as output coordinates, $\mathbf{u} = [u_1, u_2, \ldots, u_{n_u}]^T$. Then, the rest part of the coordinates is intermediate coordinates, $\mathbf{w} = [w_1, w_2, \ldots, w_{n_w}]^T$. In this paper, the collision of the structure is not considered for simplicity of the proof. Thus, the intermediate coordinates are the variables of passive joints. Therefore, there are three parts in the generalized coordinates, i.e., $\mathbf{q} = [\mathbf{u}^T, \mathbf{v}^T, \mathbf{w}^T]^T$.

In the reachable workspace, all the generalized coordinates satisfy m independent holonomic kinematic constraint equations

$$\Phi(\mathbf{q}) = \mathbf{0} \tag{7}$$

The vector function $\Phi : \mathbf{R}^{n_q} \to \mathbf{R}^m$ is a smooth function that maps n_q-dimensional real space to m-dimensional space.

For the 6-UPS discussed in this paper, the pose of the mobile platform is the output coordinates, $\mathbf{u} = [\mathbf{u}_P^T, \mathbf{u}_R^T]^T = [x, y, z, \phi, \theta, \sigma]^T$, where $\mathbf{u}_P = [x, y, z]^T$ represents position, $\mathbf{u}_R = [\phi, \theta, \sigma]^T$ represents orientation, and ϕ, θ, and σ are the parameters in T&T angles.

$\mathbf{v}$ and $\mathbf{w}$ are explicitly represented as $\mathbf{v} = \mathbf{v}(\mathbf{L}(\mathbf{u}))$ and $\mathbf{w} = \mathbf{w}(\mathbf{L}(\mathbf{u}))$. To analyze workspace, let $\mathbf{z} = [\mathbf{v}^T, \mathbf{w}^T]^T$, then $\mathbf{z} = \mathbf{z}(\mathbf{L}(\mathbf{u}))$. The corresponding function form of z is recorded as $\mathbf{\Phi}_L(\mathbf{L}(\mathbf{u}))$.

$\mathbf{z}$ is also rewritten as the component formation as follows:

$$\mathbf{z} = \left[z_1, z_2, \ldots, z_{n_v+n_w}\right]^T \tag{8}$$

There exists the following equation according to (5):

$$\mathbf{\Phi}_L(\mathbf{L}(\mathbf{u})) = \left[\Phi_L\left(\left\|\mathbf{L}_1(\mathbf{u})\right\|\right), \Phi_L\left(\left\|\mathbf{L}_2(\mathbf{u})\right\|\right), \ldots, \Phi_L\left(\left\|\mathbf{L}_{n_v+n_w}(\mathbf{u})\right\|\right)\right] \tag{9}$$

At the same time, there is

$$\left[z_1, z_2, \ldots, z_{n_v+n_w}\right] = \left[\Phi_L\left(\left\|\mathbf{L}_1(\mathbf{u})\right\|\right), \Phi_L\left(\left\|\mathbf{L}_2(\mathbf{u})\right\|\right), \ldots, \Phi_L\left(\left\|\mathbf{L}_{n_v+n_w}(\mathbf{u})\right\|\right)\right] \tag{10}$$

Therefore, we obtain the expression from (9) and (10)

$$\mathbf{\Phi}_L(\mathbf{L}(\mathbf{u})) = \left[z_1, z_2, \ldots, z_{n_v+n_w}\right] \tag{11}$$

That is, the equation is obtained from (8) and (11)

$$\mathbf{\Phi}_L(\mathbf{L}(\mathbf{u})) = \mathbf{z}^T \tag{12}$$

where $\mathbf{z}_{\min} \le \mathbf{z} \le \mathbf{z}_{\max}$.

For the poses belonging to the reachable workspace, they constitute a set Ω_A:

$$\Omega_A \equiv \left\{\mathbf{u}_P \in \mathbf{R}^3 \mid \mathbf{\Phi}_L(\mathbf{L}(\mathbf{u})) = \mathbf{z}^T; \mathbf{z}_{\min} \le \mathbf{z} \le \mathbf{z}_{\max}\right\} \tag{13}$$

In this paper, total orientation workspace is employed. Some papers analyze the workspace of 6-UPS. However, most of them choose the fixed orientation workspace in order to avoid the problem resulting from the coupling characteristic

of 6-UPS's position and orientation. This is a compromise to the computational cost. When the orientation is fixed, the problem is simplified to a 3-dimensional problem from a 6-dimensional one. Although the problem is simplified and becomes easier to solve, obviously, it does not meet the requirement of the actual working situation. Also, some researchers analyze orientation of the workspace at a fixed position, which is also not persuasive. In reality, 6-UPS with 6-DOF are required to have the ability of both translation and orientation. Therefore, a 6-dimensional workspace is necessary to be analyzed. And in this paper, the discussed workspace is total orientation workspace, i.e., all the locations of the end-effector that may be reached with all the orientations among a set defined by ranges on the orientation angles.

Total orientation workspace is defined as a set Ω_T:

$$\Omega_T \equiv \left\{ \mathbf{u}_P \in \mathbf{R}^3 \mid \mathbf{\Phi}_L(\mathbf{L}(\mathbf{u})) = \mathbf{z}^T; \mathbf{z}_{min} \le \mathbf{z} \le \mathbf{z}_{max}; \forall \mathbf{u}_R \in U_R \right\} \tag{14}$$

where U_R is the range of orientation angels in the total orientation workspace.

3. Symmetries

Three parts are involved in this section. The symmetries are proved in the first two parts. Then the symmetries are elaborated in the third part. The proof of symmetries involves the rotational symmetry around z_b-axis and the plane symmetry around the three planes perpendicular to the x_b-y_b plane of total orientation workspace. Symmetries are proved in terms of theory.

3.1. Proof of Rotational Symmetry. The structure of 6-UPS has rotational symmetry. Then, suppose the structure is rotational symmetry about z_b-axis in Figure 1 and the angle of rotation is α.

$$\begin{aligned} \mathbf{a}_{i+1} &= \mathbf{R}_z(i\alpha) \cdot \mathbf{a}_1, \\ \mathbf{b}_{i+1} &= \mathbf{R}_z(i\alpha) \cdot \mathbf{b}_1 \end{aligned} \tag{15}$$

The rotational symmetry pose of $\mathbf{u}_0$ is

$$\mathbf{u}_i' = \left[\mathbf{u}_{Pi}'^T, \mathbf{u}_{Ri}'^T \right]^T = \left[(\mathbf{R}_z(i\alpha) \cdot \mathbf{u}_P)^T, \phi + i\alpha, \theta, \sigma \right]^T \tag{16}$$

Substituting $\mathbf{u}_i'$ into (4), then

$$\begin{aligned} \left| \mathbf{L}_j(\mathbf{u}_i') \right| &= \left| \mathbf{R}_z(i\alpha) \cdot \mathbf{u}_P + \mathbf{R}_z(\phi + i\alpha) \mathbf{R}_y(\theta) \mathbf{R}_z(\sigma - \phi - i\alpha) \mathbf{a}_j - \mathbf{b}_j \right| \\ &= \left| \mathbf{R}_z(i\alpha) \cdot \left(\mathbf{u}_P + \mathbf{R}_z(\phi) \mathbf{R}_y(\theta) \mathbf{R}_z(\sigma - \phi - i\alpha) \mathbf{a}_j - \mathbf{R}_z(-i\alpha) \mathbf{b}_j \right) \right| \\ &= \left| \mathbf{R}_z(i\alpha) \cdot \left(\mathbf{u}_P + \mathbf{R}_z(\phi) \mathbf{R}_y(\theta) \mathbf{R}_z(\sigma - \phi) \mathbf{a}_{j-i+kn} - \mathbf{b}_{j-i+kn} \right) \right| = \left| \mathbf{R}_z(i\alpha) \cdot \mathbf{L}_{j-i+kn}(\mathbf{u}_0) \right| \\ &= \left| \mathbf{L}_{j-i+kn}(\mathbf{u}_0) \right| \end{aligned} \tag{17}$$

Therefore,

$$\mathbf{L}(\mathbf{u}_i') = \begin{bmatrix} 0 & 1 \\ \mathbf{E}_{n-1} & 0 \end{bmatrix}^i \cdot \mathbf{L}(\mathbf{u}_0) = \mathbf{P}^i \cdot \mathbf{L}(\mathbf{u}_0) \tag{18}$$

where k=1 or k=0 to make the subscript in the range of [1, n], $\mathbf{P}$ is the permutation matrix, and $\mathbf{E}_{n-1}$ is the n-1-dimensional identity matrix.

Therefore, according to (9) and (18)

$$\mathbf{\Phi}_L(\mathbf{L}(\mathbf{u}_i')) = \mathbf{P}^i \cdot \mathbf{\Phi}_L(\mathbf{L}(\mathbf{u}_0)) \tag{19}$$

According to (14), if the output coordinates $\mathbf{u}_0 \in \Omega_T$ and the part of orientation angles, $\mathbf{u}_{Ri}'$, in $\mathbf{u}_i'$ belongs to U_R, that is, $\mathbf{u}_{Ri}' \in U_R$, then the corresponding rotational symmetry $\mathbf{u}_i'$ also belongs to the total orientation workspace. Therefore, the rotational symmetry part is proved.

3.2. Proof of Plan Symmetry. For plane symmetry, the plane symmetry about the x_b-z_b plane passing through the line in the x_b-y_b plane $\{y = 0\}$ in Figure 1 is taken for example. According to $\mathbf{a}_i$, $\mathbf{b}_i$, the relationship of position vector between the upper and lower platform hinge points in each coordinate system is obtained

$$\begin{aligned} \mathbf{a}_{6-i+1}^L &= \mathbf{Q}\mathbf{a}_i^L \\ \mathbf{b}_{6-i+1} &= \mathbf{Q}\mathbf{b}_i \end{aligned} \tag{20}$$

where

$$\mathbf{Q} = \begin{bmatrix} 1 & 0 & 0 \\ 0 & -1 & 0 \\ 0 & 0 & 1 \end{bmatrix} \tag{21}$$

The plane symmetry pose of $\mathbf{u}_0$ is

$$\mathbf{u}_0' = \left[\mathbf{u}_{P0}'^T, \mathbf{u}_{R0}'^T \right]^T = [x, -y, z, -\phi, \theta, -\sigma]^T \tag{22}$$

For the convenience and simplicity, we assume that the structure is symmetrical about x_b-z_b plane. Two cases exist as follows. If the number of kinematic chain is even, then all A_i coordinates are as follows:

$$\begin{aligned} x_{a_1} &= x_{a_n}, \\ y_{a_1} &= -y_{a_n}, \\ z_{a_1} &= z_{a_n} \\ x_{a_2} &= x_{a_{n-1}}, \\ y_{a_2} &= -y_{a_{n-1}}, \\ z_{a_2} &= z_{a_{n-1}} \\ &\vdots \\ x_{a_{n/2}} &= x_{a_{n/2+1}}, \\ y_{a_{n/2}} &= -y_{a_{n/2+1}}, \\ z_{a_{n/2}} &= z_{a_{n/2+1}} \end{aligned} \tag{23}$$

And all B_i coordinates are as follows:

$$\begin{aligned}
x_{b_1} &= x_{b_n},\\
y_{b_1} &= -y_{b_n},\\
z_{b_1} &= z_{b_n}\\
x_{b_2} &= x_{b_{n-1}},\\
y_{b_2} &= -y_{b_{n-1}},\\
z_{b_2} &= z_{b_{n-1}}\\
&\vdots\\
x_{b_{n/2}} &= x_{b_{n/2+1}},\\
y_{b_{n/2}} &= -y_{b_{n/2+1}},\\
z_{b_{n/2}} &= z_{b_{n/2+1}}
\end{aligned} \tag{24}$$

If the number of kinematic chain is odd, then all A_i coordinates are as follows:

$$\begin{aligned}
x_{a_1} &= x_{a_{n-1}},\\
y_{a_1} &= -y_{a_{n-1}},\\
z_{a_1} &= z_{a_{n-1}}\\
x_{a_2} &= x_{a_{n-2}},\\
y_{a_2} &= -y_{a_{n-2}},\\
z_{a_2} &= z_{a_{n-2}}\\
&\vdots\\
y_{a_n} &= 0
\end{aligned} \tag{25}$$

And all B_i coordinates are as follows:

$$\begin{aligned}
x_{b_1} &= x_{b_{n-1}},\\
y_{b_1} &= -y_{b_{n-1}},\\
z_{b_1} &= z_{b_{n-1}}\\
x_{b_2} &= x_{b_{n-2}},\\
y_{b_2} &= -y_{b_{n-2}},\\
z_{b_2} &= z_{b_{n-2}}\\
&\vdots\\
y_{b_n} &= 0
\end{aligned} \tag{26}$$

The symmetrical pose about the x_b-z_b plane is $\mathbf{u}_0' = [x, -y, z, -\phi, \theta, -\sigma]^T$. Let the orientation matrix calculated using T&T angles be

$$\mathbf{R}(\phi, \theta, \sigma) = \begin{bmatrix} n_x & o_x & k_x \\ n_y & o_y & k_y \\ n_z & o_z & k_z \end{bmatrix} \tag{27}$$

Substitute $\mathbf{u}_0'$ into (27), then

$$\mathbf{R}(-\phi, \theta, -\sigma) = \begin{bmatrix} n_x & -o_x & k_x \\ -n_y & o_y & -k_y \\ n_z & -o_z & k_z \end{bmatrix} \tag{28}$$

First, we assume that the number of kinematic chains is odd. When it is even, the same result is also obtained by the similar process. Substitute $\mathbf{u}_0'$ into (4), then

$$\begin{aligned}
\mathbf{L}_i(\mathbf{u}_0') &= \begin{bmatrix} x \\ -y \\ z \end{bmatrix} + \begin{bmatrix} n_x & -o_x & k_x \\ -n_y & o_y & -k_y \\ n_z & -o_z & k_z \end{bmatrix} \begin{bmatrix} x_{a_i} \\ y_{a_i} \\ z_{a_i} \end{bmatrix} - \begin{bmatrix} x_{b_i} \\ y_{b_i} \\ z_{b_i} \end{bmatrix}\\
&= \begin{bmatrix} x \\ -y \\ z \end{bmatrix} + \begin{bmatrix} n_x & -o_x & k_x \\ -n_y & o_y & -k_y \\ n_z & -o_z & k_z \end{bmatrix} \begin{bmatrix} x_{a_{n-i+1}} \\ -y_{a_{n-i+1}} \\ z_{a_{n-i+1}} \end{bmatrix}\\
&\quad - \begin{bmatrix} x_{b_{n-i+1}} \\ -y_{b_{n-i+1}} \\ z_{b_{n-i+1}} \end{bmatrix}\\
&= \begin{bmatrix} x + n_x x_{a_{n-i+1}} + o_x y_{a_{n-i+1}} + k_x z_{a_{n-i+1}} + x_{b_{n-i+1}} \\ -\left(y + n_y x_{a_{n-i+1}} + o_y y_{a_{n-i+1}} + k_y z_{a_{n-i+1}} + y_{b_{n-i+1}}\right) \\ z + n_z x_{a_{n-i+1}} + o_z y_{a_{n-i+1}} + k_z z_{a_{n-i+1}} + z_{b_{n-i+1}} \end{bmatrix}
\end{aligned} \tag{29}$$

And there is a

$$\begin{aligned}
&\mathbf{L}_{n-i+1}(\mathbf{u}_0)\\
&= \begin{bmatrix} x + n_x x_{a_{n-i+1}} + o_x y_{a_{n-i+1}} + k_x z_{a_{n-i+1}} + x_{b_{n-i+1}} \\ y + n_y x_{a_{n-i+1}} + o_y y_{a_{n-i+1}} + k_y z_{a_{n-i+1}} + y_{b_{n-i+1}} \\ z + n_z x_{a_{n-i+1}} + o_z y_{a_{n-i+1}} + k_z z_{a_{n-i+1}} + z_{b_{n-i+1}} \end{bmatrix}
\end{aligned} \tag{30}$$

From (29) and (30), (31) is easily obtained as follows:

$$\mathbf{L}_i(\mathbf{u}_0') = \mathbf{Q}\mathbf{L}_{n-i+1}(\mathbf{u}_0) \tag{31}$$

That is,

$$\left|\mathbf{L}_i(\mathbf{u}_0')\right| = \left|\mathbf{L}_{n-i+1}(\mathbf{u}_0)\right| \tag{32}$$

Therefore,

$$\mathbf{L}(\mathbf{u}_0') = \begin{bmatrix} 0 & & 1 \\ & \iddots & \\ 1 & & 0 \end{bmatrix} \cdot \mathbf{L}(\mathbf{u}_0) = \mathbf{D} \cdot \mathbf{L}(\mathbf{u}_0) \tag{33}$$

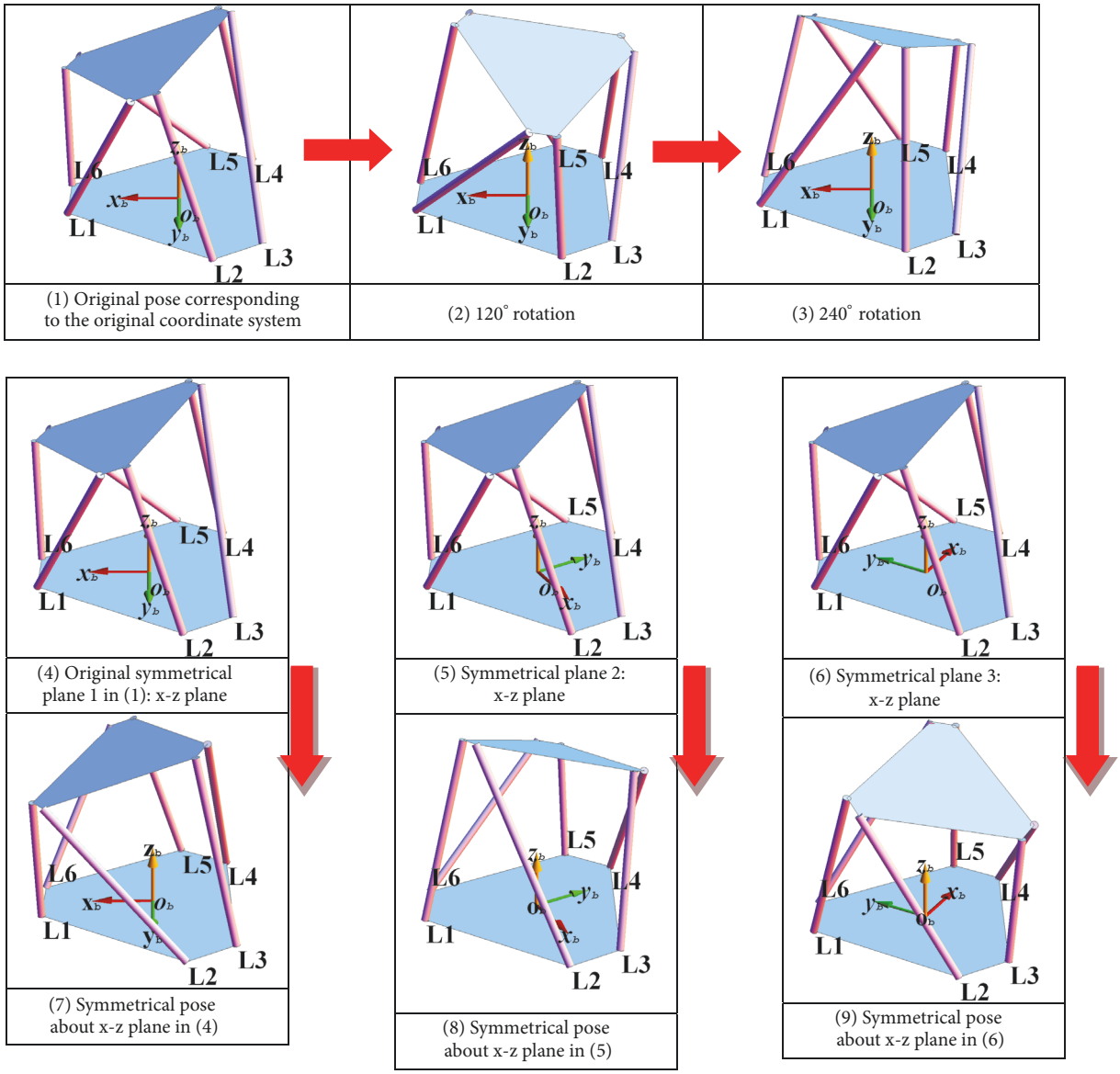

Figure 4: Five symmetrical poses.

Therefore, according to (9) and (33)

$$\Phi_L\left(L\left(u_0'\right)\right) = D \cdot \Phi_L\left(L\left(u_0\right)\right) \tag{34}$$

When the symmetry plane is the other two x_b-z_b planes in Figure 4 (5 and 6) or the number of the kinematic chains is odd, (34) is also easy to be validated in existence. According to (14), if the output coordinate $u_0 \in \Omega_T$ and the part of orientation angles, u_{R0}', in u_0' belongs to U_R, that is, $u_{R0}' \in U_R$, then the corresponding plane symmetry u_0' also belongs to the total orientation workspace. Therefore, the plane symmetry part is proved.

3.3. Analysis of Symmetries. In this section, the corresponding symmetries of workspace of the 6-UPS symmetric parallel robot are also illustrated by a practical example.

The direct pose shown in Figure 4(1) is obtained if a set of leg lengths of 6-UPS symmetric parallel robot are known. Here, the whole 6-UPS is regarded as a single rigid body. The direct pose configuration shown in Figure 4(2) is obtained when the rigid body rotates 120 degrees anticlockwise around z_b axis of the base frame. The direct pose configuration shown in Figure 4(3) is obtained when the rigid body rotates 240 degrees anticlockwise around z_b-axis of the base frame. This is called the rotational symmetry.

At the same time, the 6-UPS also has symmetries about three planes, which is called plane symmetry. The symmetrical planes include three x_b-z_b planes shown in Figure 4 (4, 5, and 6). The pose in Figure 4 (7) is the symmetrical pose about x_b-z_b plane symmetry in Figure 4 (4). The pose in Figure 4 (8) is the symmetrical pose about x_b-z_b plane symmetry in Figure 4 (5). The pose in Figure 4 (9) is the symmetrical pose about x_b-z_b plane symmetry in Figure 4 (6).

In conclusion, the five poses of the mobile platform in Figure 4 (2, 3, 7, 8, and 9) must also be the reachable pose of the 6-UPS when the pose of the mobile platform in Figure 4 (1) or Figure 4 (4) belongs to the reachable pose. It is seen that we need only to calculate a part of the workspace reasonably by using the symmetries of the workspace. Then the rest of the workspace is expressed directly according to the above principle of rotational symmetries and plane symmetries. The repeated calculation is not needed any more. Therefore, this method reduces 5/6 amount of calculation; that is, it increases the computational efficiency by 6 times.

4. Numerical Validation and Discussions

The numerical examples are performed in order to validate the correctness and validity of the symmetries of the total orientation workspace of 6-UPS about x_b-z_b plane structure symmetry.

The main idea is to prove twice rotational symmetries around z_b-axis 120° and three plane symmetries about x_b-z_b plane. The x_b-z_b plane is about one of three planes pass through the line in the x-y plane $\{y = 0\}$ in Figure 4 (4, 5, and 6), respectively. Three x_b-z_b planes are all perpendicular to the x_b-y_b plane by employing the T&T angles to represent the orientation matrix for the total orientation workspace. Finally, the results are compared with the ones caused by the orientation representation with RPY angles. The difference of the total orientation workspace calculated using T&T angles and RPY angles is presented. What is more, the correctness and effectiveness of the selected orientation representation, T&T angles, are further verified.

For numerical validation, let r_a =0.3 m, r_b =0.4 m, θ_a=0.3, θ_b=0.3, and the range of prismatic legs be [1.6, 2.6]. Thus, the vertex coordinates of the mobile and base platform of the mechanism are determined. The total orientation workspace of the 6-UPS with these structure parameters by employing the two kinds of orientation representations is analyzed below.

4.1. Workspace of Using T&T Angles. The ranges of the orientation parameters are $\phi \in (-\pi, \pi]$, $\theta \in [0, 0.6]$, and $\sigma \in [-0.6, 0.6]$.

Through discretization method, the points cloud and a section plane at z=1.8 of the workspace are shown in Figures 5(a) and 5(b).

The workspace of the 6-UPS has the same symmetry with its structure seen from the points cloud.

For example, there is a pose $\mathbf{u}_0 = [0.5, 0.6, 1.9, 0.2, 0.3, 0.4]^{\mathrm{T}}$ and the orientation matrix is as follows:

$$\mathbf{R}_0 = \begin{pmatrix} 0.87816 & -0.380722 & 0.289629 \\ 0.380722 & 0.922824 & 0.0587108 \\ -0.289629 & 0.0587108 & 0.955336 \end{pmatrix} \tag{35}$$

By the inverse kinematics, we get

$$\mathbf{L}(\mathbf{u}_0) = [2.0096, 2.0358, 2.0740, 2.1695, 2.1457, 1.9637] \tag{36}$$

According to (16), the two rotational symmetries poses about the z_b-axis are as follows:

$$\begin{aligned} \mathbf{u}_1' &= [-0.7696, 0.1330, 1.9, 2.2944, 0.3, 0.4]^{\mathrm{T}} \\ \mathbf{u}_2' &= [0.2696, -0.7330, 1.9, 4.3888, 0.3, 0.4]^{\mathrm{T}} \end{aligned} \tag{37}$$

Combining with (1) and (3) we also get

$$\begin{aligned} &\mathbf{L}(\mathbf{u}_1') = [2.1457, 1.9637, 2.0096, 2.0358, 2.0740, 2.1695] \\ &\mathbf{L}(\mathbf{u}_2') = [2.0740, 2.1695, 2.1457, 1.9637, 2.0096, 2.0358] \end{aligned} \tag{38}$$

From (36) and (38), it is easily found that

$$\mathbf{L}(\mathbf{u}_2') = \mathbf{P}^2 \cdot \mathbf{L}(\mathbf{u}_1') = \mathbf{P}^4 \cdot \mathbf{L}(\mathbf{u}_0) \tag{39}$$

This is the same as (18).

As for plane symmetry, for the structure of 6-UPS in Fig, only consider the symmetry about the x_b-z_b plane. Therefore, $\mathbf{u}_0' = [0.5, -0.6, 1.9, -0.2, 0.3, -0.4]^{\mathrm{T}}$, and the lengths of legs are obtained by (1) and (3):

$$\mathbf{L}(\mathbf{u}_0') = [1.9637, 2.1457, 2.1695, 2.0740, 2.0358, 2.0096] \tag{40}$$

From (36) and (40), the relation of (33) exists, i.e.,

$$\mathbf{L}(\mathbf{u}_0') = \begin{bmatrix} 0 & & 1 \\ & \iddots & \\ 1 & & 0 \end{bmatrix} \cdot \mathbf{L}(\mathbf{u}_0) = \mathbf{D} \cdot \mathbf{L}(\mathbf{u}_0) \tag{41}$$

Thus, the numerical example is consistent with the theory.

4.2. Workspace of Using RPY Angles. Here, let the ranges of the parameters of RPY angles to be $\phi \in [-0.6, 0.6]$, $\theta \in [-0.6, 0.6]$, and $\sigma \in [-0.6, 0.6]$.

Also the points cloud and a section plane at z=1.8 of the workspace are calculated and drawn, as shown in Figures 6(a) and 6(b), through discretization method.

Figure 6 shows that the total orientation workspace is symmetrical only about x_b-z_b plane. Even in certain cases, a pose is in the workspace, while its symmetrical pose is not. Therefore, the orientation is difficult to be represented by RPY angles. Moreover, the total orientation workspace does not possess the rotational symmetry characteristic as the structure.

In conclusion, the proof of symmetries of the total orientation workspace has been finished. The numerical examples verify the symmetrical characteristics of workspace influenced by the choice of orientation representation. Here, the choice of T&T angles leads to the corresponding symmetrical workspace with the symmetrical structure, while the one of RPY angles does not.

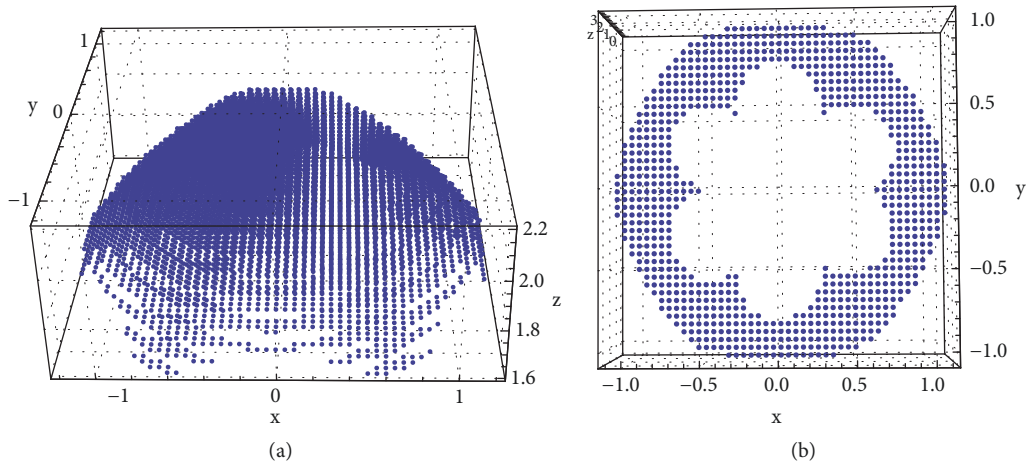

Figure 5: Total orientation workspace using T&T angles.

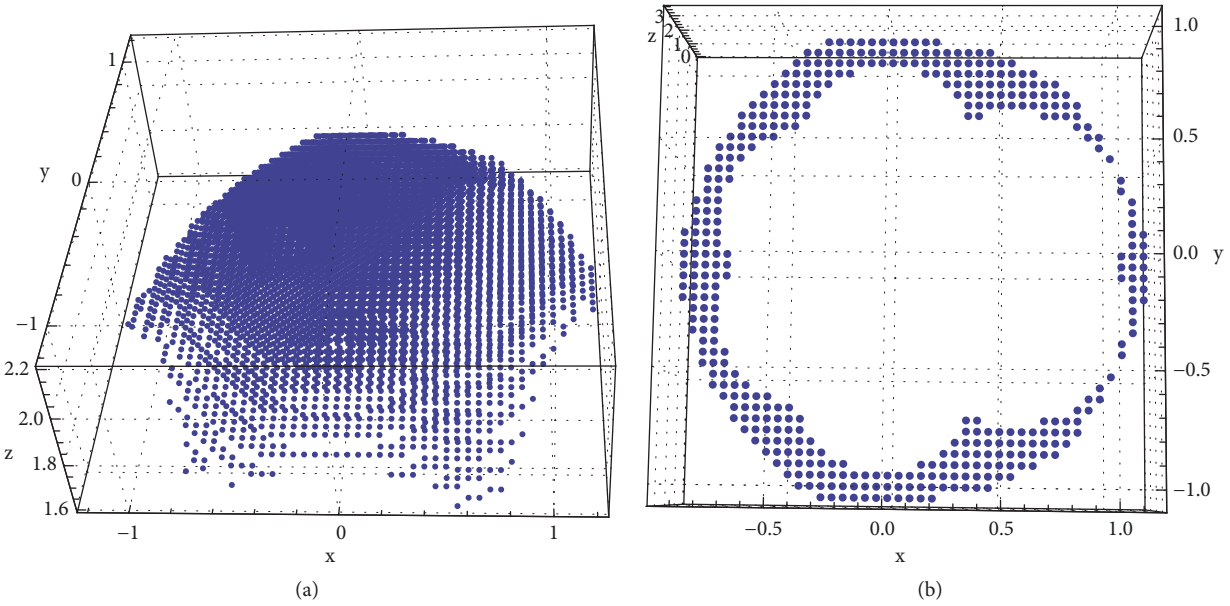

Figure 6: Total orientation workspace using RPY angles.

5. Conclusions and Future Work

(1) T&T angles are found and provide favorable conditions for the symmetry proof. T&T angles are beneficial for representing the orientation matrix of the mobile platform of 6-UPS.

(2) Total orientation workspace of 6-UPS is obtained by the discrete algorithm. The total orientation workspace is proved to possess symmetrical characteristics, consistent with the structural symmetry of 6-UPS.

(3) Computation cost is reduced 5/6 due to the symmetrical characteristics of the total orientation workspace of 6-UPS and the computational efficiency is increased by 6 times when analyzing 6-UPS.

(4) The further study will focus on the advantages of symmetries in the field of singularity, kinematics, and dynamics.

Data Availability

The data used to support the findings of this study are available from the corresponding author upon request.

Conflicts of Interest

The authors declared no potential conflicts of interest with respect to the research, authorship, and/or publication of this article.

Acknowledgments

The authors disclosed receipt of the following financial support for the research, authorship, and/or publication of this article: this research is supported by the Natural Science

Research of Jiangsu Higher Education Institutions of China (Grant no. 17KJB460003), the National Natural Science Foundation of China (Grants nos. 51375230 and 51705243), and the Natural Science Foundation of Jiangsu Province (Grant no. BK20170789). The authors gratefully acknowledge these support agencies.

References

[1] P. J. Merlet, *Parallel Robots*, vol. 128, Springer Science & Business Media, 2006.

[2] Y. Lou, G. Liu, N. Chen et al., "Optimal design of parallel manipulators for maximum effective regular workspace," *IEEE/RSJ International Conference on Intelligent Robots and Systems*, pp. 795–800, 2005.

[3] T. Huang, B. Jiang, and D. J. Whitehouse, "Determination of the carriage stroke of 6-PSS parallel manipulators having the specific orientation capability in a prescribed workspace," *IEEE International Conference on Robotics and Automation*, vol. 3, pp. 2382–2385, 2000.

[4] J. Blaise, I. Bonev, B. Monsarrat, S. Briot, J. M. Lambert, and C. Perron, "Kinematic characterisation of hexapods for industry," *Industrial Robot*, vol. 37, no. 1, pp. 79–88, 2010.

[5] J. S. Zhao, M. Chen, K. Zhou, J. X. Dong, and Z. J. Feng, "Workspace of parallel manipulators with symmetric identical kinematic chains," *Mechanism & Machine Theory*, vol. 41, no. 6, pp. 632–645, 2006.

[6] J.-S. Zhao, F. Chu, and Z.-J. Feng, "Symmetrical characteristics of the workspace for spatial parallel mechanisms with symmetric structure," *Mechanism and Machine Theory*, vol. 43, no. 4, pp. 427–444, 2008.

[7] S. Durango, D. Restrepo, O. Ruiz, J. Restrepo-Giraldo, and S. Achiche, "Symmetrical observability of kinematic parameters in symmetrical-parallel mechanisms," *Blucher Mechanical Engineering Proceedings*, vol. 1, pp. 254–272, 2010.

[8] I. A. Bonev and C. M. Gosselin, "Analytical determination of the workspace of symmetrical spherical parallel mechanisms," *IEEE Transactions on Robotics*, vol. 22, no. 5, pp. 1011–1017, 2006.

[9] Q. Jiang and C. M. Gosselin, "Evaluation and representation of the theoretical orientation workspace of the Gough-Stewart platform," *Journal of Mechanisms and Robotics*, vol. 1, no. 2, Article ID 021004, pp. 1–9, 2009.

[10] J. J. Craig, *Introduction to Robotics: Mechanics and Control*, vol. 3, Pearson Prentice Hall, Upper Saddle River, NJ, USA, 2005.

[11] I. A. Zlatanov and D. Gosselin, "Advantages of the modified Euler angles in the design and control of PKMs," in *Proceedings of the Parallel Kinematic Machines International Conference*, 2002.

[12] I. A. Bonev and J. Ryu, "New approach to orientation workspace analysis of 6-DOF parallel manipulators," *Mechanism and Machine Theory*, vol. 36, no. 1, pp. 15–28, 2001.

[13] T. Huang, J. Wang, and D. J. Whitehouse, "Closed form solution to workspace of hexapod-based virtual axis machine tools," *Journal of Mechanical Design*, vol. 121, no. 1, pp. 26–31, 1999.

[14] N. R. Crawford, G. T. Yamaguchi, and C. A. Dickman, "A new technique for determining 3-D joint angles: the tilt/twist method," *Clinical Biomechanics*, vol. 14, no. 3, pp. 153–165, 1999.

[15] I. A. Bonev and C. M. Gosselin, "Singularity loci of spherical parallel mechanisms," in *Proceedings of the IEEE International Conference on Robotics and Automation*, pp. 2957–2962, April 2005.

[16] J.-S. Zhao, F. Chu, and Z.-J. Feng, "Singularities within the workspace of spatial parallel mechanisms with symmetric structures," *Proceedings of the Institution of Mechanical Engineers, Part C: Journal of Mechanical Engineering Science*, vol. 224, no. 2, pp. 459–472, 2010.